

**Biomimetic zeolite for the removal of heavy metal ions and harmful dye from  
wastewater**

**S.Sandiyashini**

**Krithika Udayasankar**

## Abstract

The effectiveness of various treatments in enhancing the adsorption capacity of zeolite for the removal of  $\text{Cu}^{2+}$  and  $\text{Pb}^{2+}$  and methylene blue dye (MB) was studied and the results were used to construct a working water filtration prototype for wastewater treatment. Clinoptilolite was treated with either citric acid (zeo-C) or sodium dodecyl sulfate (zeo-S) or a combination of both (zeo-CS). The zeolite adsorbent dose was kept at 10 g/L for the adsorption of MB dye and  $\text{Cu}^{2+}$  and  $\text{Pb}^{2+}$  ions. The most effective adsorbent was zeo-S, followed by zeo-CS, followed by zeo-C. The adsorption equilibrium data for zeo-S fitted well to Langmuir isotherm. Subsequently, a prototype consisting of a floating device and ‘tentacles’ that contain zeo-S was constructed. 3 different ways to contain zeo-S was tested to investigate the best way to contain zeolite in order to maximise adsorption: stainless steel metal infusers (MI), teabags (TB) and a hybrid combination of MI and TB designs where one tea bag was placed inside a tea infuser (HY). The HY design had the highest adsorption capacity in adsorbing heavy metal ions and MB due to its ability to contain 2 layers of zeolite, thus increasing the number of monolayer adsorption sites exposed to the adsorbate solution. Zeo-s is found to be a very viable, low cost and effective adsorbent that can be built into a sustainable wastewater treatment device.

## 1. Introduction

One of the main contributors to water pollution is improperly treated discharge of industrial wastewater. It contains pollutants, like heavy metal ions and textile dyes, which can give rise to many negative implications if not properly treated. For example, the discharging of toxic dye effluents into the aqueous environment takes up dissolved oxygen needed by aquatic life and is toxic to microbial organisms and potentially carcinogenic to mammals [1]. The heavy metal ions cause detrimental health effects -  $\text{Cu}^{2+}$  ions inhibit  $\text{Na}^+$  channels on human epithelial cells [2] and  $\text{Pb}^{2+}$  ions disrupt synaptic activity in human bodies [3]. While several alternatives such as

activated carbon have been studied, they are not cost-effective for use in rural communities where water pollution and untreated wastewater discharge is more extensive. [4]

Zeolite is a low-cost adsorbent that has been extensively used in gaseous exchange studies [5-7]. Studies have also reported the effectiveness of zeolite in organic dye removal [8-10] and heavy metal ion removal [11-13] from wastewater. Furthermore, several treatment methods to optimise the adsorption capacity of zeolites using organic surfactants [10, 14] and acids [15, 16] have been studied. Organic surfactant treatment reduces the surface tension of the liquid, thereby potentially allowing dye and heavy metal ions to penetrate the microporous surface of the zeolite more effectively. In particular, sodium dodecyl sulfate (SDS) treated adsorbents have been proved to be the most effective surfactant for cationic dye adsorption in the study by Jin et al. [10]. Acid treatment potentially increases the amount of Bronsted acid sites on zeolite surfaces [10] and dealuminates the zeolite structure [15]. Notably, citric acid (CA) has relatively high stability among acids, and significantly improved the adsorption capacity of zeolite [16, 17]. However, little has been done to comparatively analyse the different treatment methods to increase zeolite’s adsorption capacity and translate its theoretical adsorption effectiveness into working prototypes.

This study aims to compare the effectiveness of various treatments in enhancing the adsorption capacity of zeolite and utilise the findings to construct a working wastewater treatment prototype. Clinoptilolite was chosen to be studied as it is the most abundant and naturally occurring zeolite. Its good resistance to temperature and ionizing radiations also makes it suitable to construct a sturdy prototype. In this study, clinoptilolite was treated with either CA or SDS or a combination of both to adsorb common heavy metal ions,  $\text{Cu}^{2+}$  and  $\text{Pb}^{2+}$ , and methylene blue dye (MB). A working water filter was then constructed using the treated zeolite with the highest adsorption capacity.

## **2. Materials and Method**

### Preparation of Zeolite

High purity zeolite containing 90-95% clinoptilolite was purchased from Hydrolab®, washed with distilled water and oven dried at 100 °C for 24 h before being pounded and sieved to particles with a size range of 500-2000 µm. This zeolite was then treated with 3% SDS or 0.3 M CA or a mixed solution of 3% SDS solution and 0.3 M CA. After 24 hours of treatment with shaking at 250 rpm, the zeolite was washed with distilled water and oven dried at 100 °C for 24 h. The SDS treated zeolite, CA treated zeolite, SDS and CA treated zeolite and untreated zeolite were labelled as zeo-S, zeo-C, zeo-CS and zeo-U respectively. The pH of all zeolite was maintained at approximately 6.

### Characterisation of zeolite

A Joel, JSM-6010LA analytical scanning electron microscope was used to study the morphology of zeo-S, zeo-C, zeo-CS and zeo-U. BET (Brunauer–Emmett–Teller) analysis of resolution 0-50 nm was done using Quantachrome Autosorb 1 analyzer in a certified lab (Latech Scientific Supply, Singapore) to study the pore size, pore volume and pore surface area of the zeolite samples.

### Preparation of Adsorbate

Cu<sup>2+</sup> and Pb<sup>2+</sup> solutions of concentrations 200, 400, 600, 800 and 1000 ppm, and MB solutions of concentrations 40, 80, 120, 160 and 200 ppm were prepared by diluting from 10 000 ppm stock solution. The UV-Vis Spectrophotometer, Shimadzu UV-1240, was used to measure the absorbance value of MB solutions at 665 nm which corresponds to the maximum absorbance of MB to plot a calibration curve. The R<sup>2</sup> values for the calibration curves were kept above 0.995.

### Adsorption Studies

First, the effect of initial concentration of adsorbate on the adsorption capacity of zeolite was studied. 0.4 g of zeolite was added to 40 ml of adsorbate at the varied concentrations of heavy metal ions and dyes as stated

above and shaken for 2 hours at 250 rpm. At the end of the studies, adsorbent was filtered off from the adsorbate. The initial concentration (C) and final concentration (C<sub>0</sub>) after adsorption of Cu<sup>2+</sup> and Pb<sup>2+</sup> solutions were measured using the PerkinElmer Atomic Absorption Spectroscopy (AAS) machine while that of MB was measured via the Spectrophotometer at 665 nm and compared against the calibration curve for final concentration. The percentage adsorption was calculated by [C<sub>0</sub> - C] / C<sub>0</sub> x 100%.

The same adsorbent to adsorbate ratio was then used in the equilibrium studies where equilibrium concentration (C<sub>e</sub>) and equilibrium adsorption capacity of zeolite (Q<sub>e</sub>) were measured with the contact time of 24 hours. The results were analysed the same way as the prior concentration studies. The following linearised equations were used to fit our results from this study into the isotherms:

$$\text{Langmuir Isotherm: } C_e/Q_e = (1/K_L)Q_m + C_e/Q_m$$

$$\text{Freundlich Isotherm: } \log(Q_e) = \log(K_F) + 1/n (\log(C_e))$$

### Filtration Prototype design and testing

A device was designed to contain zeo-S which will be used to treat untreated polluted water. The prototype consists of multiple tentacle-like features each containing zeolite substrate. These ‘arms’ are attached to a floating material which allows the prototype to experience neutral buoyancy, allowing our prototype to move along with the water currents smoothly such that it can be removed once zeo-S are fully saturated. The design is modelled after the biostructure of sea anemones, and the device, similar to the filter feeding mechanism of sea anemones [18, 19], filters untreated wastewater and ‘feeds’ on adsorbates via its ‘arms’. It is designed to meet the following criteria: adjustability of the length of each individual arm to adapt to different depths of water or varying densities of pollutants, ease of replacing used zeolites in the device, cost effectiveness, adaptability of device possibly by designing it to be an extension of existing structures such as floating platforms, as well as sustainability such that there is no disruption of aquatic ecosystems.



**Figure 1 Types of prototype designs tested: (from Left to Right) Teabags (TB), Stainless Steel metal tea infusers (MI), Hybrids (HY)**

3 different ways to contain the zeolite were tested: Stainless steel metal infusers (MI), teabags (TB) and a Hybrid combination of MI and TB designs to form 2 layers of zeolite, where one tea bag was placed inside a tea infuser (HY) were each attached to a pool float. The pool float was made of recycled granulated closed cell foam and measured approximately 15 by 25 cm. The MI and TB designs each held 1.5 g of zeo-S, while the HY design had each component containing 0.75 g of zeo-S separately. Figure 1.1 shows the 3 different

options that were tested to find out the best prototype design that would maximise adsorption by zeo-S. 2 samples of each design were made, with one batch acting as controls with no zeolite. The samples were placed inside beakers containing 40 ppm MB solution and 200 ppm Cu<sup>2+</sup> and Pb<sup>2+</sup> combined solution and shaken for 24 h at 150 ppm.

### 3. Results and Discussion

#### Characterisation of zeolite

As seen from Table 2, zeo-C has the largest surface area (36.1 m<sup>2</sup>/g), followed by zeo-U (29.8 m<sup>2</sup>/g) and zeo-C (25.2 m<sup>2</sup>/g). This suggests that the adsorption capacity of zeo-C is the largest due to a larger adsorption site available for the adsorbate molecules. The mean pore diameter of zeo-S (17.2 nm) is the largest, followed by zeo-U (14.7 nm) and zeo-C (13.3 nm). This corroborates with the SEM images of zeolite. In Figure S1, zeo-S appears to be the most porous with its micropore being the most well-defined, thereby also potentially contributing to an increased surface area for a larger number micropores to adsorb the pollutant molecules. On the other hand, zeo-C seems to have extensive coating with a smoother and

even texture, with less-defined micropore. This extensive coating caused by acid treatment could have filled up the zeolite's natural pore structure, resulting in a smaller micropore diameter.

**Table 2 Surface area, pore volume and mean pore diameter of zeo-U, zeo-C and zeo-S**

Type of zeolite	zeo-U	zeo-C	zeo-S
BET surface area (m <sup>2</sup> /g)	29.8	36.1	25.2
BJH Adsorption average pore diameter (nm)	14.7	13.3	17.2

#### Effect of concentration and varying treatment of zeolite on removal of MB, Cu<sup>2+</sup> and Pb<sup>2+</sup> ions

As seen from Figure 3, amongst the four types of zeolites, zeo-S was the most effective at removing MB, with adsorption capacity of 13.6 mg/g, which is double of that of zeo-CS (7.81 mg/g) and zeo-U (7.18 mg/g) and triple of that of zeo-C (4.42 mg/g). Its high adsorption capacity can be explained by SDS' anionic nature due to its SO<sup>4</sup><sup>-</sup> group, which is complementary to the positively charged MB molecule as seen in Figure 3. This allows zeo-S to have a greater affinity for MB dye molecules. SDS treated zeolite by Jin et al. [10] showed similar adsorption capacities to zeo-S, within the range of 12-13 mg/g for MB .

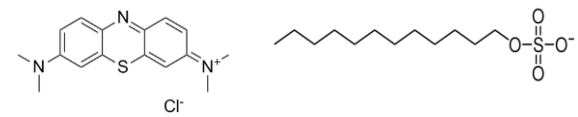


**Figure 3 Molecular structure of SDS (left) and MB (right)**

Also, in Figure 4, the largest rate of increase in adsorption capacity was observed at the highest initial concentration of MB, possibly due to the largest driving force of dye molecules to overcome limited mass transport of MB onto zeolite adsorption sites [10].

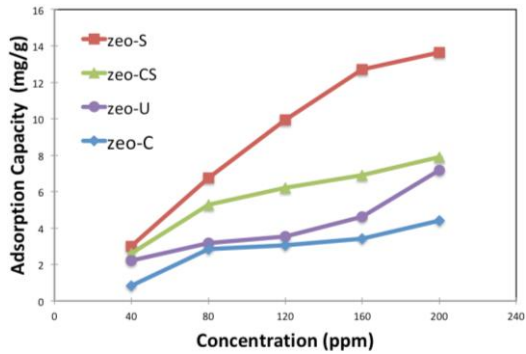


*Figure 4 Effect of concentration and varying treatment of zeolite on removal of MB dye in 2h. Error bars represent standard deviation for technical triplets.*

As seen from Figure 5, zeo-S was the most effective at removing  $\text{Pb}^{2+}$  ions, with adsorption capacity of 47.6 mg/g, followed by zeo-CS (35.9 mg/g), zeo-U (33.6 mg/g) and zeo-C (28.3 mg/g). Zeolite samples adsorbed about 65-70% less  $\text{Cu}^{2+}$  ions as compared to  $\text{Pb}^{2+}$  ions at the 5 different initial concentrations. As seen from Figure 5, zeo-S was still the most effective at removing  $\text{Cu}^{2+}$  ions with the highest adsorption capacity of 14.2 mg/g in a 200 ppm solution, followed by zeo-CS (8.80 mg/g), zeo-C (6.08 mg/g) and zeo-U (7.36 mg/g).

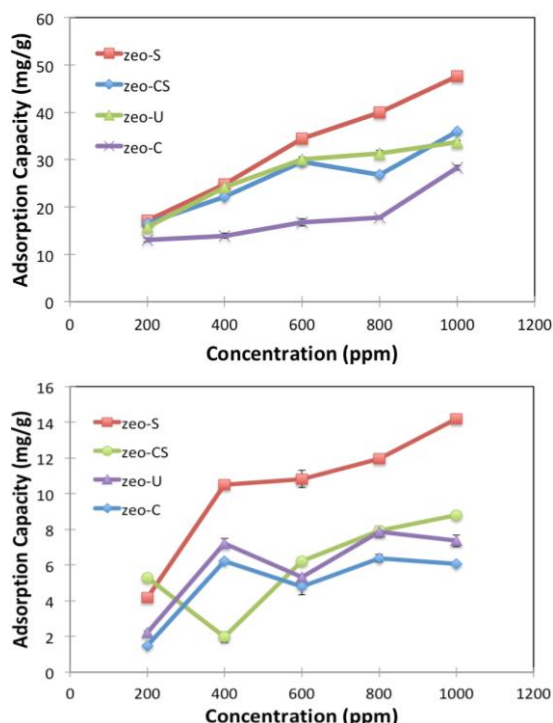


*Figure 5 Effect of concentration and varying treatment of zeolite on removal of  $\text{Pb}^{2+}$  ions (left) and  $\text{Cu}^{2+}$  ions (right) in 2h. Error bars represent standard deviation for technical triplets.*

Zeo-C consistently achieves the lowest adsorption capacity. This is most likely due to the room temperature 0.3M CA treatment which failed to decationise zeolite to exchange zeolite's unstable cations with  $\text{H}^+$  ions, thus not making zeolite porous enough to allow for greater adsorption capacity. CA treatment at higher temperatures should be considered for future work. This correlates with the BJH Adsorption average pore diameter trend which shows that zeo-C has the smallest pore diameter, thus reducing its adsorption capacity. This also aligns with the SEM images, as the micropores should be clogged, thus reducing the pore size available for adsorbate molecules.

### Isotherms

Both the Langmuir and Freundlich adsorption isotherms describe the adsorption mechanism of the interaction of MB molecules,  $\text{Cu}^{2+}$  and  $\text{Pb}^{2+}$  ions on the surface of zeolite. As seen from Figure S2, the adsorption isotherm of zeolite can be fitted onto the Langmuir model for all 3 adsorbates, with correlation coefficient  $R^2 > 0.96$ . This corroborates with a study on zeolite that found its MB adsorption mechanism to be in accordance with the Langmuir model [20] and a study on clinoptilolite where it experienced a similar fit to the Langmuir model for the adsorption of heavy metal ions such as  $\text{Cu}^{2+}$ ,  $\text{Zn}^{2+}$ ,  $\text{Fe}^{3+}$  and  $\text{Mn}^{2+}$ . [21]

Hence, the adsorption mechanism of zeolite confirms the 4 assumptions of the Langmuir model:

1. The MB molecules,  $\text{Cu}^{2+}$  and  $\text{Pb}^{2+}$  ions are adsorbed at definite sites on the surface of zeolite.
2. Each site can accommodate only one MB molecule or  $\text{Cu}^{2+}$  and  $\text{Pb}^{2+}$  ion (monolayer).
3. The area of each site is a fixed quantity determined solely by the geometry of the surface.
4. The adsorption energy is the same at all the adsorption sites.

Compared to studies with experimental data that also fit the Isotherm model, zeo-S has a higher maximum adsorption capacity ( $Q_m$ ) for  $\text{Cu}^{2+}$  (21.1 mg/g) than

natural zeolite (3.37 mg/g). Zeo-S also has a higher  $Q_m$  for MB (20.1 mg/g) as compared to zeolite fly ash (14.3 mg/g) [22] and silica (11.2 mg/g) [23]. Zeo-S has a significantly higher  $Q_m$  for  $Pb^{2+}$  (75.2 mg/g) as compared to activated carbon synthesised from sea-buckthorn stones (25.9 mg/g) [24] and commercial activated carbon (23.4 mg/g) [25]. Overall, zeo-S has performed better across the 3 adsorbates as compared to the other treatments.

#### Effect of prototype design on the adsorption of MB

From Figure 6, all 3 prototypes show similar adsorption capacities ranging from 19.6 mg/g to 19.7 mg/g. However, the hybrid design shows the highest adsorption capacity of 19.7 mg/g. As the prototype follows the Langmuir Isotherm, the hybrid prototype's formation of a double layer model (with the steel mesh forming one and the tea bag forming another inner layer) may allow the zeolite to adsorb a greater amount of dyes as a greater number of monolayers are present.

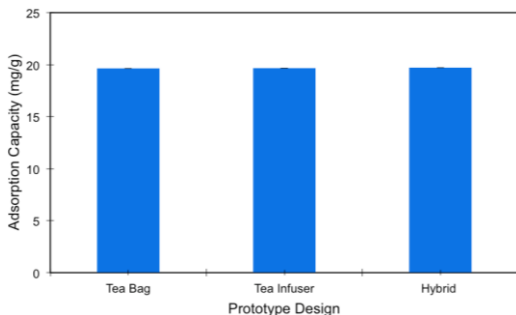


Figure 6 Bar graph showing the effect of prototype design on the adsorption of MB dye. Error bars represent standard deviation for technical triplets.

#### Effect of prototype design on the adsorption of $Pb^{2+}$ and $Cu^{2+}$ ions

From Figure 7, all 3 prototypes show similar adsorption capacities of  $Pb^{2+}$  and  $Cu^{2+}$  ions ranging from 18.9 mg/g to 19.0 mg/g. The hybrid design shows the highest adsorption capacity of 19.0 mg/g. From the graph, it can be observed that in both TB and MI designs, the adsorption capacity of  $Pb^{2+}$  ions (19.0 mg/g), is almost twice as much as  $Cu^{2+}$  ions (10.1 mg/g, 9.75 mg/g). In HY design, the difference between adsorption capacities of  $Pb^{2+}$  (19.0 mg/g) and  $Cu^{2+}$  ions (17.1 mg/g) is much less significant as there is a notable increase in the adsorption capacity of  $Cu^{2+}$  ions. When compared to Figure 5, it can

be seen that the adsorption capacity values are similar in both combined and single ion solutions and the pattern of adsorption capacities across the heavy metal ions remain the same. The viability of the prototype is proven by the combined solution of  $Pb^{2+}$  and  $Cu^{2+}$  displaying similar adsorption capacities to single solution adsorption capacities.

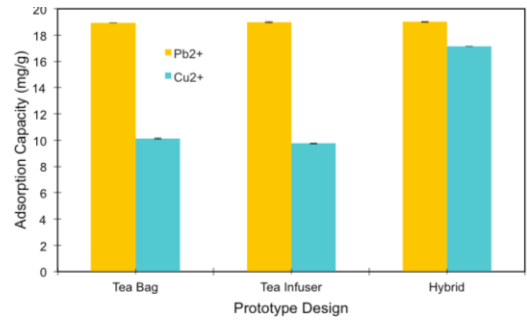


Figure 7 Bar graph showing the effect of prototype design on the adsorption of  $Pb^{2+}$  and  $Cu^{2+}$  ions. Error bars represent standard deviation for technical triplets.

## 4. Conclusion

In this study, zeo-S, zeo-C and zeo-CS has been successful in adsorption of MB and heavy metal ions, with zeo-S having the highest adsorption capacity for  $Pb^{2+}$ ,  $Cu^{2+}$  and MB. The adsorption of MB and heavy metal ions onto zeo-S fits the Langmuir isotherm, indicating that the zeolite adsorption is a monolayer coverage. 3 variations of zeolite prototypes were constructed and their varying adsorption capacities were tested with a combined  $Pb^{2+}$  and  $Cu^{2+}$  solution and MB solution. The HY design had the highest adsorption capacity for the adsorption of all 3 pollutants. The results of this study yields the possibility of developing an electrokinetic remediation device [26] that incorporates natural minerals such as zeolites as well as other soil remediation and industrial wastewater treatment devices. More study can also be carried out in optimising the treatment processes for the zeolites to customise their adsorption capacities of various adsorbates as required by different polluted water bodies, such as but not limited to the concentration of SDS treatment and the temperature of the acid treatment.

## References

- [1] Chequer, F. M. D., Oliveira, G. A. R. de, Ferraz Elisa Raquel Anastácio, Cardoso, J. C., Zanoni, M. V. B., & Oliveira, D. P. de. (2013, January 16). Textile Dyes: Dyeing Process and Environmental Impact. Retrieved from <https://www.intechopen.com/books/eco-friendly-textile-dyeing-and-finishing/textile-dyes-dyeing-process-and-environmental-impact>
- [2] Chen, J., Myerburg, M. M., Passero, C. J., Winarski, K. L., & Sheng, S. (2011, August 5). External Cu<sup>2+</sup> inhibits human epithelial Na channels by binding at a subunit interface of extracellular domains. Retrieved from <https://www.ncbi.nlm.nih.gov/pmc/articles/PMC3149337/>
- [3] Gorkhali, R., Huang, K., Kirberger, M., & Yang, J. J. (2016, June 1). Defining potential roles of Pb(2+) in neurotoxicity from a calciumomics approach. Retrieved from <https://www.ncbi.nlm.nih.gov/pmc/articles/PMC4979543/>.
- [4] [https://www.researchgate.net/publication/222544093\\_Impact\\_of\\_Water\\_Pollution\\_on\\_Rural\\_Communities\\_An\\_Economic\\_Analysis](https://www.researchgate.net/publication/222544093_Impact_of_Water_Pollution_on_Rural_Communities_An_Economic_Analysis)
- [5] Aoki, K., Tuan, V. A., Falconer, J. L., & Noble, R. D. (2000, September 28). Gas permeation properties of ion-exchanged ZSM-5 zeolite membranes. Retrieved from <https://www.sciencedirect.com/science/article/abs/pii/S1387181100002249>
- [6] Ackley, M. W., Giese, R. F., & Yang, R. T. (2004, August 23). Clinoptilolite: Untapped potential for kinetics gas separations. Retrieved from <https://www.sciencedirect.com/science/article/abs/pii/01442499290050Y>
- [7] Kuehl, G. H., & Timken, H. K. C. (2000, April 6). Acid sites in zeolite Beta: effects of ammonium exchange and steaming. Retrieved from <https://www.sciencedirect.com/science/article/abs/pii/S1387181199002474>
- [8] Wang, S., & Zhu, Z. H. (2006, February 28). Characterisation and environmental application of an Australian natural zeolite for basic dye removal from aqueous solution. Retrieved from <https://www.sciencedirect.com/science/article/abs/pii/S0304389406000495>
- [9] Meshko, V., Markovska, L., Mincheva, M., & Rodrigues, A. E. (2001, July 31). Adsorption of basic dyes on granular activated carbon and natural zeolite. Retrieved from <https://www.sciencedirect.com/science/article/abs/pii/S043135401000562>
- [10] Jin, X., Jiang, M.-qin, Shan, X.-quan, Pei, Z.-guo, & Chen, Z. (2008, October 9). Adsorption of methylene blue and orange II onto unmodified and surfactant-modified zeolite. Retrieved from <https://www.sciencedirect.com/science/article/abs/pii/S0021979708010904#bib001>
- [11] Kocaoba, S. (2009, June 9). Adsorption of Cd(II), Cr(III) and Mn(II) on natural sepiolite. Retrieved from <https://www.sciencedirect.com/science/article/abs/pii/S011916409002914>
- [12] Blanchard, G., Maunaye, M., & Martin, G. (2003, April 4). Removal of heavy metals from waters by means of natural zeolites. Retrieved from <https://www.sciencedirect.com/science/article/abs/pii/0043135484901246>
- [13] Ćurković, L., Cerjan-Stefanović, Š., & Filipan, T. (1998, July 25). Metal ion exchange by natural and modified zeolites. Retrieved from <https://www.sciencedirect.com/science/article/abs/pii/S0043135496004113>
- [14] Li, Z., Burt, T., & Bowman, R. S. (2000). Sorption of Ionizable Organic Solutes by Surfactant-Modified Zeolite. *Environmental Science & Technology*, 34(17), 3756–3760. Retrieved from <https://pubs.acs.org/doi/abs/10.1021/es990743o>
- [15] Zaiku, X., Qingling, C., Chengfang, Z., Jiaqing, B., & Yuhua, C. (2000). Influence of Citric Acid Treatment on the Surface Acid Properties of Zeolite Beta. *The Journal of Physical Chemistry B*, 104(13), 2853–2859. doi: 10.1021/jp991471e
- [16] Junbo Xu, Nie Xin, Jian Li, Lina Yang. “The acid treatments of the H $\beta$  zeolite as the catalyst in the synthesis of ethyl tertiary butyl ether antiknock additive.” *International Journal of Advancements in Research & Technology*. (2013, December) Retrieved from <http://www.ijoart.org/docs/The-acid-treatments-of-the-H%2C3%9F-zeolite-as-the-catalyst.pdf>

- [17] ZHANG, B.-hua, WU, D.-yi, WANG, C., HE, S.-bing, ZHANG, Z.-jia, & KONG, H.-nan. (2007, June 1). Simultaneous removal of ammonium and phosphate by zeolite synthesized from coal fly ash as influenced by acid treatment. Retrieved from <https://www.sciencedirect.com/science/article/pii/S1001074207600904>
- [18] Mitchelmore, C. L., Verde, E. A., Ringwood, A. H., & Weis, V. M. (2003). Differential accumulation of heavy metals in the sea anemone *Anthopleura elegantissima* as a function of symbiotic state. *Aquatic Toxicology*, 64(3), 317–329. doi: 10.1016/s0166-445x(03)00055-9
- [19] Rubenstein, D. I., & Koehl, M. A. R. (1977). The Mechanisms of Filter Feeding: Some Theoretical Considerations. *The American Naturalist*, 111(981), 981–994. Retrieved from <https://www.journals.uchicago.edu/doi/abs/10.1086/283227>
- [20] Rida, K., Bouraoui, S., & Hadnine, S. (2013). Adsorption of methylene blue from aqueous solution by kaolin and zeolite. *Applied Clay Science*, 83-84, 99–105. doi: 10.1016/j.clay.2013.08.015
- [21] M. B. (2008). Adsorption of Heavy Metals from Aqueous Solutions on Synthetic Zeolite. *Research Journal of Environmental Sciences*, 2(1), 13–22. doi: 10.3923/rjes.2008.13.22
- [22] Shah, B. A., Shah, A. V., & Patel, H. D. (2011). Alkaline hydrothermal conversion of agricultural waste Bagasse Fly Ash into zeolite: utilisation in dye removal from aqueous solution. Retrieved from <http://www.inderscience.com/offer.php?id=37376>
- [23] Woolard, C. D., Strong, J., & Erasmus, C. R. (2002, February 12). Evaluation of the use of modified coal ash as a potential sorbent for organic waste streams. Retrieved from <https://www.sciencedirect.com/science/article/abs/pii/S0883292702000574>
- [24] Mohammadi, S. Z., Karimi, M. A., Afzali, D., & Mansouri, F. (2010). Removal of Pb(II) from aqueous solutions using activated carbon from Sea-buckthorn stones by chemical activation. *Desalination*, 262(1-3), 86–93. Retrieved from <https://pillbuys.com/research/Sea buckthorn oil/19.pdf>
- [25] Rahman, Adil, Mohd, Yusof, Ansary, & H., R. (2014, May 7). Removal of Heavy Metal Ions with Acid Activated Carbons Derived from Oil Palm and Coconut Shells. Retrieved from <https://www.mdpi.com/1996-1944/7/5/3634/htm>
- [26] Elsayed-Ali, A. H., Abdel-Fattah, T., & Elsayed-Ali, H. E. (2011). Laboratory Experiment on Electrokinetic Remediation of Soil. *Journal of Chemical Education*, 88(8), 1126–1129. doi: 10.1021/ed1008766
- [27] Nassar, M. Y., Abdelrahman, E. A., Aly, A. A., & Mohamed, T. Y. (2017). A facile synthesis of mordenite zeolite nanostructures for efficient bleaching of crude soybean oil and removal of methylene blue dye from aqueous media. *Journal of Molecular Liquids*, 248, 302–313. doi: 10.1016/j.molliq.2017.10.061
- [28] Singh, S., Sidhu, G. K., & Singh, H. (2017). Removal of methylene blue dye using activated carbon prepared from biowaste precursor. *Indian Chemical Engineer*, 1–12. doi: 10.1080/00194506.2017.1408431
- [29] Geçgel, Ü., Özcan, G., & Gürpinar, G. Ç. (2013). Removal of Methylene Blue from Aqueous Solution by Activated Carbon Prepared from Pea Shells (*Pisum sativum*). *Journal of Chemistry*, 2013, 1–9. doi: 10.1155/2013/614083